Hindawi Publishing Corporation
Journal of Sensors
Volume 2013, Article ID 650572, 7 pages
http://dx.doi.org/10.1155/2013/650572

Research Article

Growth and Characterization of Single Crystalline $Bi_4Ge_3O_{12}$ Fibers for Electrooptic High Voltage Sensors

Stephan Wildermuth,[1,2] Klaus Bohnert,[1] Hubert Brändle,[1] Jean-Marie Fourmigue,[3] and Didier Perrodin[3]

[1] *ABB Switzerland Ltd., Corporate Research, Segelhof 1K, 5405 Baden-Dättwil, Switzerland*
[2] *ABB AG, Corporate Research, Wallstadter Straße 59, 68526 Ladenburg, Germany*
[3] *Fibercryst, S.A.S., La Doua-Bat L'Atrium, Boulevard, Latariet, 69616 Villeurbanne Cedex, France*

Correspondence should be addressed to Stephan Wildermuth; stephan.wildermuth@de.abb.com

Received 26 February 2013; Accepted 1 June 2013

Academic Editor: Kiyoshi Kurosawa

The micro-pulling-down technique for crystalline fiber growth is employed to grow fibers and thin rods of bismuth germanate, $Bi_4Ge_3O_{12}$ (BGO), for use in electrooptic high voltage sensors. The motivation is the growth of fibers that are considerably longer than the typical lengths (100–250 mm) that are achieved by more conventional growth techniques like the Czochralski technique. At a given voltage (several hundred kilovolts in high voltage substation applications) longer sensors result in lower electric field strengths and therefore more compact and simpler electric insulation. BGO samples with lengths up to 850 mm and thicknesses from 300 μm to 3 mm were grown. Particular challenges in the growth of BGO fibers are addressed. The relevant optical properties of the fibers are characterized, and the electrooptic response is investigated at voltages up to 30 kV_{rms}.

1. Introduction

Voltage and current measurements are two key functions in the control and protection of electric power grids. Traditionally voltage is measured by means of inductive instrument transformers or capacitive voltage dividers. Such transformers have been state of the art for many decades but have also a number of drawbacks. In particular they represent heavy and space consuming equipment (with weights of up to several tons at the highest voltage levels). In recent years optical sensors for high voltage and current have found considerable attention as attractive alternatives. Advantages of optical voltage sensors over conventional voltage transformers include higher fidelity (e.g., due their larger bandwidth and absence of effects like ferroresonances), smaller weight and size, inherent galvanic isolation of secondary electronics from high voltage, and reduced environmental impact (e.g., no risk of oil spills). Furthermore, their output is readily compatible with the modern digital equipment for substation control and protection.

Commonly optical voltage sensors make use of the electrooptic effect (Pockels effect) in materials such as bismuth germanium oxide, $Bi_4Ge_3O_{12}$ (BGO), or bismuth silicon oxide, $Bi_4Si_3O_{12}$ (BSO) [1–5]. Several sensor configurations have been reported. In gas-insulated high voltage switchgear a small electrooptic crystal may be integrated into a capacitive voltage divider where it measures a small fraction of the line voltage [2–4]. In an optical voltage transducer for air-insulated substations reported in [5] the voltage is derived from several local electric field measurements at different positions along a path from ground to high voltage. The crystals are placed inside a nitrogen-filled insulator column with provisions for maintaining a stable electric field distribution and reducing the effects of stray fields. In [6, 7], lithium niobate-based electrooptic waveguides were investigated for high voltage measurement as an alternative to bulk crystals.

Potentially more accurate are sensors that measure not only a fraction of the power line voltage but the total voltage. Here, the full line voltage of up to 550 kV is applied to a BGO crystal with a length of 100–200 mm [8, 9]. Since the method

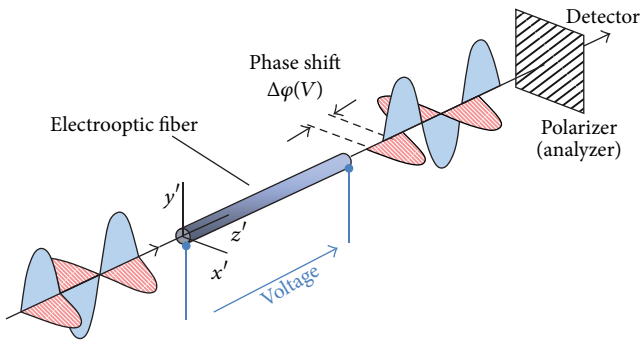

Figure 1: Electrooptic voltage measurement.

Table 1: Crystal classes (in Hermann-Mauguin notation) without natural birefringence suited for line integration of the electric field.

Class	Axis parallel to light propagation	Direction of electrooptical axes	Materials
$\bar{4}3m$	$\bar{4}$-fold axis [001]	[110]	$Bi_4Ge_3O_{12}$ $Bi_4Si_3O_{12}$ ZnTe, ZnSe, GaAs
$\bar{4}2m$	$\bar{4}$-fold axis [001]	[110]	KH_2PO_4 (KDP)
23	2-fold axis [001]	[110]	$NaClO_3$

results in high electric field strengths around the crystal, the sensor is mounted in an insulator of relatively large diameter in order to keep the field outside the insulator below critical limits for electric breakdown and partial discharge in air. SF_6 gas under pressure prevented the internal dielectric breakdown.

Electrically poled fused-silica fibers were also investigated for voltage measurement [10, 11]. The poling lifts the centrosymmetry of fused silica and introduces a linear electrooptic effect. In principle, a transversally poled fiber appropriately arranged along a helical path allows one to integrate the electric field over an extended distance from ground to high voltage. However, the required long-term stability of the poling and other difficulties pose serious challenges. Alternatively the line voltage may be applied to a quartz crystal or partitioned onto a series of crystals. The piezo-electric deformation of the crystals is sensed by a means of a white light fiber interferometer [12, 13]. A high voltage sensor using piezo-electric ceramics and interrogation by means of a fiber Bragg grating was reported in [14].

In the present paper we report on the growth and characterization of BGO electrooptic fibers and thin rods and explore their potential for high voltage measurement. Here, a particular motivation is the growth of fibers that are considerably longer than the typical lengths (100–250 mm) that are achieved by more conventional growth techniques like the Czochralski technique. At a given voltage (several hundred kilovolts in high voltage substation applications) longer sensors result in lower electric field strengths and therefore make possible more compact and less expensive electric insulation. Furthermore, the fiber is to measure the line integral of the electric field in order to make the sensor insensitive to stray fields from neighboring power lines. The fibers are grown using the so-called micro-pulling-down (μ-PD) technique [15, 16]. The μ-PD method was developed to grow single crystal fibers from materials such as Nd:$Y_3Al_5O_{12}$ (Nd:YAG) or Al_2O_3 (sapphire) for use in fiber lasers [17, 18], crystalline scintillator fibers for medical imaging [19–21], and fluoride fibers.

The paper is organized as follows: in Section 2 we determine the electrooptic crystal classes that are suitable for measuring the path integral of the electric field. In Section 3 we describe the micro-pulling-down (μ-PD) technique and some particular challenges in the growth of BGO fibers. The characterization of the BGO samples is presented in Section 4 followed by some conclusions.

2. Optical Voltage Measurement by Path Integration of the Electric Field

The voltage V between two points A and B is defined as the path integral of the electric field along an arbitrary path from A to B:

$$V = \int_A^B \vec{E}\, d\vec{s}. \tag{1}$$

A voltage sensor that measures this path integral is not affected by stray fields from neighboring power lines and changes in the electric field distribution, for example, as a result of weather conditions or nearby structures. A corresponding sensor must linearly respond to the electric field and only be sensitive to field components parallel to the integration path.

Figure 1 shows the basic concept of an electrooptic voltage measurement. Two orthogonal light waves propagate through the electrooptic material (along z-axis) with polarization directions parallel to the electrooptic axes (x', y'). As a result of the birefringence induced by an applied electric field the two waves accumulate a phase difference $\Delta\varphi$ in proportion to the field strength. An analysis of the electrooptic (i.e., noncentrosymmetric) crystal classes yields several classes that meet the conditions for a path integration of the field [22, 23]; that is, only the field component parallel to the optical path in Figure 1 shall cause an electrooptic phase shift whereas transverse components shall leave the phase difference unaffected.

Table 1 lists the three suitable classes that are free of natural birefringence and indicates for each class the crystal axis that must be aligned parallel to the light propagation direction and the direction of the electrooptic axes. Furthermore, examples of materials are given. Table 2 lists two suitable classes that are naturally birefringent. In those classes the principal axes of the natural and electrooptic birefringence coincide. There are further classes which may also be suitable for field integration but where the axes of natural and field-induced birefringence do not coincide. Those classes are not considered here. Note that symmetry properties of the piezoelectric effect in certain crystal classes can also be employed to measure the path integral of the electric field with an optical sensor [24, 25].

Table 2: Crystal classes with natural birefringence suited for line integration of the electric field.

Class	Axis parallel to light propagation	Direction of electrooptical axes	Materials
$\bar{6}2$m	2-fold axis	[110]	$LiNaCO_3$
2 mm	2-fold axis	[110]	KPT, $KNbO_3$

Figure 2: Electrooptic BGO voltage sensor in 170 kV gas-insulated switchgear. The BGO crystal is inside the transparent insulator tube between the electrodes at high voltage (bottom) and ground potential (top). The crystal is operated in a reflective mode with optical fiber cables (red) guiding the light to and from the ground potential side.

We have chosen BGO ($Bi_4Ge_3O_{12}$) of the $\bar{4}3$m symmetry class as a material for fiber growth as it is already well known for electrooptic voltage sensing in form of bulk crystals, and initial experience in the growth of BGO fibers for scintillator purposes was already available [20]. Figure 2 shows an example of a bulk BGO crystal sensor. It is a 170 kV voltage sensor for integration in gas-insulated high voltage switchgear developed during some of our earlier work (unpublished). BGO is free of natural birefringence; that is, there is no offset to the electrooptic phase shift which could vary with temperature. In contrast to the compound semiconductor materials listed in Table 1, BGO has a sufficiently small electric conductivity within the typical temperature range of operation (−40 to 85°C) [26]. Another advantage is the moderate dependence of the electrooptic effect on temperature ($1.54{\cdot}10^{-4}$°C^{-1}) [27].

According to Table 1, a 4-fold crystal axis [001] must be aligned parallel to the optical path in z-direction (corresponding to the longitudinal fiber axis in case of a BGO fiber). The electrooptic axes x' and y' are oriented along the crystallographic [110]-directions. The electrooptic phase retardation is given as

$$\Delta\varphi = \frac{2\pi}{\lambda} n_o^3 r_{41} V. \quad (2)$$

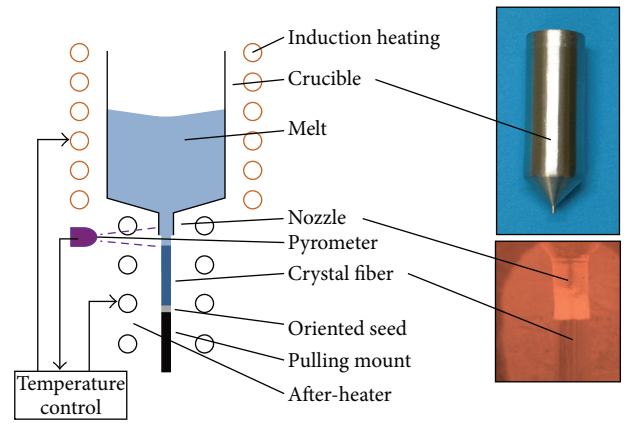

Figure 3: Left: schematics of the micro-pulling-down apparatus for BGO fiber growth. Top right: photograph of the platinum crucible. Bottom right: CCD image of the crystallization zone during crystal growth.

Here, λ is the wavelength of operation, $n_o = 2.098$ is the refractive index, and $r_{41} = 0.96$ pm/V is the relevant electrooptic coefficient. The resulting half-wave voltage $V_\pi = \lambda/(2n_o^3 r_{41})$ is 73.9 kV at a wavelength of 1310 nm [26].

3. BGO Fiber Growth by Micro-Pulling-Down Technique

As mentioned in the introduction the μ-PD technique is of interest for the growth of thin crystalline fibers, particularly for use in lasers and scintillator devices. BGO fibers have been grown for application in medical imaging devices [19–21]. In this context the goal was to cut a BGO fiber of small cross section into small pixels for high spatial resolution. In contrast, we explore in the following the μ-PD technique for its suitability to grow long crystalline BGO fibers and thin rods with optical quality sufficient for voltage sensing.

The μ-PD setup is schematically shown in Figure 3. The molten material resides in a platinum crucible with inductive heating. The melt flows downwards through a microcapillary at the bottom of the crucible and crystallizes below the exit nozzle. The crystallization starts at a seed crystal which determines the crystal orientation. The seed crystal is pulled downwards at a controlled speed. In the present investigations the melt was made of BGO material grown by the Czochralski method. Growth from mixtures of Bi_2O_3 and Ge_2O_2 powders was investigated in preceding work [20]. The growth process was optimized with regard to good optical quality of the BGO fiber and homogeneous growth over extended length. In contrast to sapphire or YAG fibers the growth of BGO fibers turned out to be rather sensitive to the stability and magnitude of the capillary nozzle temperature. Conductive heat flow as well as thermal emission varies as a function of the melt level in the crucible and the grown fiber length, thus influencing the growth process. Particularly at longer grown fiber lengths there was a substantial heat loss through the fiber as a result of BGO's high thermal conductivity and transparency to infrared radiation. Therefore an extra

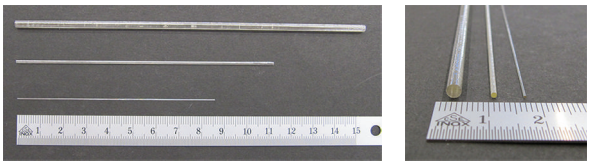

Figure 4: BGO fibers fabricated by the micro-pulling-down technique. The aspect ratio of the BGO fibers from top to bottom is 50, 112, and 172, respectively.

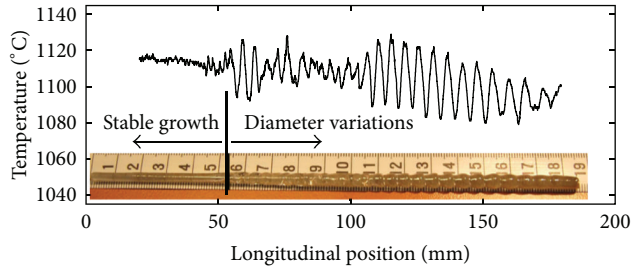

Figure 5: Effect of variations in crucible capillary temperature on BGO sample thickness. The BGO solidification temperature is 1050°C.

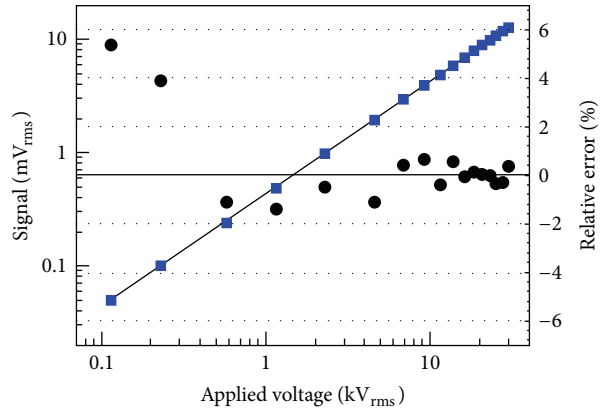

Figure 6: Electrooptic signal from a 150 mm long BGO sample versus applied alternating voltage (squares) and relative deviation from a linear fit (dots).

after-heater combined with a precise pyrometer in a feedback loop was employed to control and stabilize the temperature in the crystallization zone. The heater also reduced thermal gradients and served to anneal the crystallized material to minimize imperfections and stress. A ceramics enclosure around the crucible (not shown in Figure 3) ascertained good thermal isolation and temperature homogeneity. Another particular complication is Bi_2O_3 evaporation from the melt which, if not prevented, changes the melt composition during the growth process. The evaporation was minimized by a sufficiently tight enclosure which led to a Bi_2O_3 saturated atmosphere. For a given nozzle size the fiber diameter was controlled via the pull-down speed of the seed crystal (typically 0.5–1 mm/min). A CCD camera allowed monitoring the fiber growth in situ.

4. Results and Discussion

The grown BGO fibers and thin rods had diameters in the range of 300 μm to 3 mm and lengths of up to 850 mm (Figure 4). The maximum length was limited by the growth equipment. Figure 5 illustrates the importance of the temperature control. In order to achieve a homogeneous fiber thickness the capillary temperature had to be kept stable within about 5°C. Too low temperatures led to crystallization of the melt at the crucible's nozzle making the fiber bend. On the other hand, too high temperatures led to melt overflow at the nozzle and caused the fiber diameter to increase beyond the nozzle diameter. The overflow is caused by the high wettability of the BGO melt on platinum. Possibly other crucible materials such as iridium or molybdenum could be alternatives.

Due to the mentioned difficulties it was not possible to grow extended length of fiber without small bends or buckles. The longest buckle-free fiber sections had lengths between 150 mm and 200 mm. A visual inspection of the samples indicated good optical quality without obvious defects. The absorption coefficient was measured at 633 nm (HeNe laser) for 18 samples from three different growth runs with a length from 2.1 cm to 16.5 cm. The beam waist was kept smaller than the sample diameter in order to avoid influences from the outer surface. Taking into account the losses at the end faces due to Fresnel reflection the resulting absorption coefficients were in the range of $<0.005\,cm^{-1}$ to $0.045\,cm^{-1}$ with the majority of samples near $0.01\,cm^{-1}$. The absorption was essentially independent of the sample thickness. For comparison, recently reported data for conventionally grown bulk material were in the range of $0.0005\,cm^{-1}$ to $0.03\,cm^{-1}$ [28].

The following results were obtained from a thin BGO rod with a length of 150 mm and a diameter of 3 mm. The sample birefringence was measured in order to quantitatively examine built-in stress and defects from the growth process (as mentioned crystals of class $\bar{4}3m$ which include BGO are free of natural birefringence). The birefringent phase retardation was determined to be 0.6 rad (34°) at a wavelength of 1310 nm. The corresponding average birefringence Δn is $0.83{\cdot}10^{-8}$. For comparison, the birefringent phase retardation of high quality BGO crystals of similar length grown by the Czochralski method was found to be about 0.1-0.2 rad. The direction of the principal axes of the birefringence was essentially constant over the sample length, indicated by the fact that linear light polarization along this direction was well preserved. An X-ray examination of selected samples indicated that the crystal orientation was largely uniform along the samples.

Figure 6 shows the electrooptic response of the sample in a configuration as shown in Figure 2. Two parallel electrode plates with openings for the crystal ends were used to apply a variable AC voltage of 60 Hz in the longitudinal crystal direction. The light from a 1310 nm superluminescent diode was linearly polarized with the polarization aligned for maximum electrooptic signal (polarization at 45° to electrooptic axes). A Soleil-Babinet compensator behind the crystal compensated the mentioned birefringent phase retardation and was adjusted to introduce an overall phase bias of 90° between

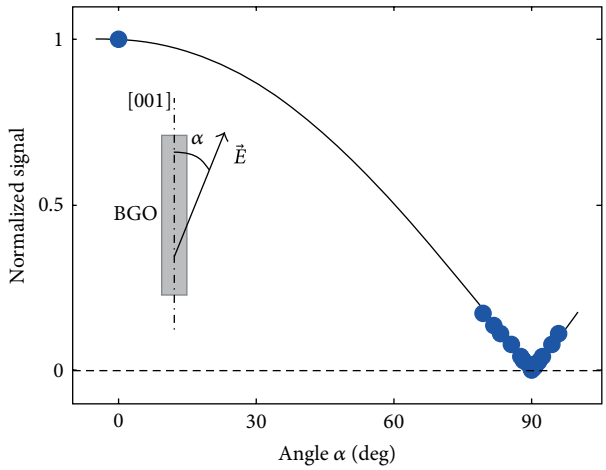

FIGURE 7: Electrooptic signal (normalized amplitude) versus electric field direction α (dots) for a Czochralski-grown reference BGO crystal. The longitudinal crystal axis coincides with a 4-fold crystal axis, [001]-direction.

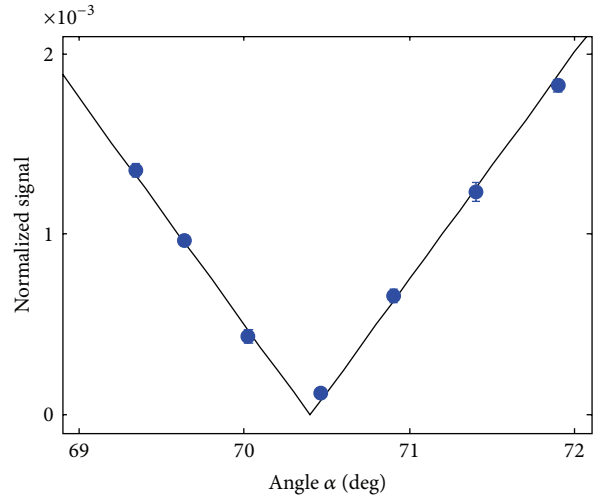

FIGURE 8: Electrooptic signal versus electric field direction α for a BGO sample grown by the μ-PD technique at a fixed azimuth angle of the field. The minimum is displaced from 90° indicating a misalignment of the crystal axes.

the two orthogonal polarization components. A polarizer after the compensator converted the electrooptic phase shift into an intensity change. The detected signal is then given as

$$S = S_o \left[1 + \varsigma \sin\left(\frac{\pi V}{V_\pi}\right)\right]. \quad (3)$$

S_o is proportional to the light source power, and ς is the fringe contrast. The signal increased linearly with a voltage up to the maximum voltage of 30 kV_{rms} (Figure 6). Obviously the nonlinear range of (3) was not yet reached which indicated that the electrooptic phase shift was smaller than expected for the V_π-voltage of bulk BGO (73.9 kV at 1310 nm). In part we attribute this to the fact that the orientation of the crystal axes deviated from the nominal orientation as seen in the following. Figure 7 shows the electrooptic signal as a function of the direction α of a homogeneous electric field for a cylinder-shaped Czochralski-grown reference crystal. The crystal length and diameter were 60 mm and 5 mm, respectively. The crystal orientation was again according to Table 1. α was the angle between the field direction and the long crystal axis. The signal amplitude followed as expected the absolute value of the cosine of α (independent of the field azimuth angle), which confirmed that the crystal measures only the field component along the longitudinal crystal axis. Figure 8 shows the equivalent data for the sample grown by the μ-PD method at a fixed azimuth angle. Here, the signal minimum was shifted by 19.6° from $\alpha = 90°$ to $\alpha = 70.4°$ indicating a misalignment of the crystallographic axes. The misalignment was confirmed in subsequent X-ray diffraction measurements on several samples where angular deviations of the [001]-direction from the longitudinal crystal axis between 20° and 25° were found. Possibly, the deviation was caused by misalignment of the seed crystal at the start of the growth process. On the other hand in some of the investigated samples the X-ray measurements allowed to distinguish two superimposed diffraction patterns characteristic for crystal twins. This indicates that the orientation of the crystal varied along a given sample which cannot only be attributed to a misalignment of the seed crystal.

5. Conclusion and Outlook

The micro-pulling-down technique was used to grow optical fibers of single crystalline $Bi_4Ge_3O_{12}$ with a length of up to 850 mm and diameters between 300 μm and 3 mm. In general, the grown material was of a reasonably good optical quality. The measurement of high voltages with such fibers was demonstrated. Nevertheless, the growth of fibers from BGO by the μ-PD technique turned out to be rather challenging compared to growth of fibers from other materials such as sapphire or YAG. Further improvements of the control of the growth process, the thermal management, and possibly use of other materials for the crucible will be necessary to achieve a more homogeneous growth over extended lengths.

Furthermore, the investigated BGO fibers did not yet have a core/cladding structure for guided wave operation. Multimode wave-guiding may be achieved by a polymer cladding equivalently to hard clad silica fibers. Since BGO has a substantially higher refractive index ($n = 2.1$ at 1310 nm) than fused silica, high refractive index polymers would be preferred. Such polymers have been of interest for optoelectronic applications. By adding metal oxides like titanium oxide or zirconium oxide to the polymer, refractive indices as high as 1.9 have been achieved [29]. Another option to increase the refractive index is the addition of compound semiconductor nanoparticles, for example, from ZnS to the polymer [30].

The most preferred solution is a fiber with a crystalline core and a crystalline cladding. Such fibers can be grown with the μ-PD technique by employing two concentric crucibles that contain appropriately doped melts of a given material. In [31], for example, lithium niobate fibers with Mn-doped

cladding were reported. Possible dopants for BGO include rare earth and metals ions such as Ce, Nd, Sm, Tb, Ho, Er, Cr, Mn, or Fe [32].

Acknowledgment

The authors would like to thank Professor O. Tillement from Lyon 1 University, France, for the support and discussions.

References

[1] K. Shibata, "A fiber optic electric field sensor using the electro-optic effect of $Bi_4Ge_3O_{12}$," in *Proceedings of the 1st International Conference on Optical Fibre Sensors*, vol. 221, pp. 164–168, London, UK, April 1983.

[2] T. Mitsui, K. Hosoe, H. Usami, and S. Miyamoto, "Development of fiber-optic voltage sensors and magnetic field sensors," *IEEE Transactions on Power Delivery*, vol. 2, no. 1, pp. 87–93, 1987.

[3] T. Sawa, K. Kurosawa, T. Kaminishi, and T. Yokota, "Development of optical instrument transformers," *IEEE Transactions on Power Delivery*, vol. 5, no. 2, pp. 884–891, 1990.

[4] S. Kobayashi, A. Horide, I. Takagi et al., "Development and field test evaluation of optical current and voltage transformers for gas insulated switchgear," *IEEE Transactions on Power Delivery*, vol. 7, no. 2, pp. 815–821, 1992.

[5] P. P. Chavez, F. Rahmatian, and N. A. F. Jaeger, "Accurate voltage measurement with electric field sampling using permittivity-shielding," *IEEE Transactions on Power Delivery*, vol. 17, no. 2, pp. 362–368, 2002.

[6] N. A. F. Jaeger and L. Young, "High-voltage sensor employing an integrated optics Mach-Zehnder interferometer in conjunction with a capacitive divider," *Journal of Lightwave Technology*, vol. 7, no. 2, pp. 229–235, 1989.

[7] N. A. F. Jaeger and F. Rahmatian, "Integrated optics pockels cell high-voltage sensor," *IEEE Transactions on Power Delivery*, vol. 10, no. 1, pp. 127–134, 1995.

[8] C. P. Yakymyshyn, M. A. Brubaker, P. M. Johnston, and C. Reinbold, "Manufacturing challenges of optical current and voltage sensors for utility applications," in *Sensors and Controls for Advanced Manufacturing*, vol. 3201 of *Proceedings of SPIE*, pp. 2–19, 1997.

[9] K. Bohnert, P. Gabus, H. Brändle, and A. Khan, "Fiber-optic current and voltage sensors for high-voltage substations," in *Proceedings of the 16th International Conference on Optical Fiber Sensors*, pp. 752–754, 2003.

[10] P. G. Kazansky, P. S. J. Russell, and H. Takebe, "Glass fiber poling and applications," *Journal of Lightwave Technology*, vol. 15, no. 8, pp. 1484–1493, 1997.

[11] A. Michie, I. Bassett, and J. Haywood, "Electric field and voltage sensing using thermally poled silica fibre with a simple low coherence interferometer," *Measurement Science and Technology*, vol. 17, no. 5, pp. 1229–1233, 2006.

[12] K. Bohnert, M. Ingold, and J. Kostovic, "Fiber-optic voltage sensor for SF6 gas-insulated high-voltage switchgear," *Applied Optics*, vol. 38, no. 10, pp. 1926–1933, 1999.

[13] K. Bohnert, J. Kostovic, and P. Pequignot, "Fiber optic voltage sensor for 420 kV electric power systems," *Optical Engineering*, vol. 39, no. 11, pp. 3060–3067, 2000.

[14] R. C. Allil and M. M. Werneck, "Optical high-voltage sensor based on fiber bragg grating and PZT piezoelectric ceramics," *IEEE Transactions on Instrumentation and Measurement*, vol. 60, no. 6, pp. 2118–2125, 2011.

[15] D.-H. Yoon, I. Yonenaga, T. Fukuda, and N. Ohnishi, "Crystal growth of dislocation-free $LiNbO_3$ single crystals by micro pulling down method," *Journal of Crystal Growth*, vol. 142, no. 3-4, pp. 339–343, 1994.

[16] A. Yoshikawa and V. Chani, "Growth of optical crystals by micro-pulling-down method," *MRS Bulletin*, vol. 34, no. 4, pp. 266–270, 2009.

[17] H. S. Fang, Z. W. Yan, and E. D. Bourret-Courchesne, "Numerical study of the micro-pulling-down process for sapphire fiber crystal growth," *Crystal Growth and Design*, vol. 11, no. 1, pp. 121–129, 2011.

[18] V. I. Chani, A. Yoshikawa, Y. Kuwano, K. Hasegawa, and T. Fukuda, "Growth of $Y_3Al_5O_{12}$:Nd fiber crystals by micro-pulling-down technique," *Journal of Crystal Growth*, vol. 204, no. 1, pp. 155–162, 1999.

[19] J. B. Shim, J. H. Lee, A. Yoshikawa, M. Nikl, D. H. Yoon, and T. Fukuda, "Growth of $Bi_4Ge_3O_{12}$ single crystal by the micro-pulling-down method from bismuth rich composition," *Journal of Crystal Growth*, vol. 243, no. 1, pp. 157–163, 2002.

[20] V. Chani, K. Lebbou, B. Hautefeuille, O. Tillement, and J.-M. Fourmigue, "Evaporation induced diameter control in fiber crystal growth by micro-pulling-down technique: $Bi_4Ge_3O_{12}$," *Crystal Research and Technology*, vol. 41, no. 10, pp. 972–978, 2006.

[21] M. Zhuravleva, V. I. Chani, T. Yanagida, and A. Yoshikawa, "The micro-pulling-down growth of $Bi_4Si_3O_{12}$ (BSO) and $Bi_4Ge_3O_{12}$ (BGO) fiber crystals and their scintillation efficiency," *Journal of Crystal Growth*, vol. 310, no. 7–9, pp. 2152–2156, 2008.

[22] K. Bohnert and J. Nehring, "Method and device for the optical determination of a physical quantity," U.S. Patent 5,715,058, 1998.

[23] L. Duvillaret, S. Rialland, and J.-L. Coutaz, "Electro-optic sensors for electric field measurements. II. Choice of the crystals and complete optimization of their orientation," *Journal of the Optical Society of America B*, vol. 19, no. 11, pp. 2704–2715, 2002.

[24] K. Bohnert and J. Nehring, "Fiber-optic sensing of electric field components," *Applied Optics*, vol. 27, no. 23, pp. 4814–4818, 1988.

[25] K. Bohnert and J. Nehring, "Fiber-optic sensing of voltages by line integration of the electric field," *Optics Letters*, vol. 14, pp. 290–292, 1989.

[26] G. Montemezzani, St. Pfändler, and P. Günter, "Electro-optic and photorefractive properties of $Bi_4Ge_3O_{12}$ crystals in the ultraviolet spectral range," *Journal of the Optical Society of America B*, vol. 9, pp. 1110–1117, 1992.

[27] P. A. Williams, A. H. Rose, K. S. Lee, D. C. Conrad, G. W. Day, and P. D. Hale, "Optical, thermo-optic, electro-optic, and photoelastic properties of bismuth germanate ($Bi_4Ge_3O_{12}$)," *Applied Optics*, vol. 35, no. 19, pp. 3562–3569, 1996.

[28] V. D. Golyshev, M. A. Gonik, and V. B. Tsvetovsky, "Spectral absorptivity and thermal conductivity of BGO and BSO melts and single crystals," *International Journal of Thermophysics*, vol. 29, no. 4, pp. 1480–1490, 2008.

[29] T. D. Flaim, Y. Wang, and R. Mercado, "High refractive index polymer coatings for optoelectronics applications," in *Advances in Optical Thin Films*, vol. 5250 of *Proceedings of SPIE*, 2004.

[30] C. Lü, Z. Cui, Y. Wang et al., "Preparation and characterization of ZnS-polymer nanocomposite films with high refractive index," *Journal of Materials Chemistry*, vol. 13, no. 9, pp. 2189–2195, 2003.

[31] B. M. Epelbaum, K. Inaba, S. Uda et al., "A double-die modification of micro-pulling-down method for in situ clad/core doping of fiber crystal," *Journal of Crystal Growth*, vol. 179, no. 3-4, pp. 559–566, 1997.

[32] S. G. Raymond, B. J. Luff, P. D. Townsend, X. Feng, and G. Hu, "Thermoluminescence spectra of doped $Bi_4Ge_3O_{12}$," *Radiation Measurements*, vol. 23, no. 1, pp. 195–202, 1994.